Published OnlineFirst April 11, 2014; DOI: 10.1158/1078-0432.CCR-14-0107

Translational Relevance

Oncogene fusions, such as the *ALK*, *RET*, and *ROS1* fusions, have recently been revealed as therapeutic targets in lung adenocarcinoma (LDAC). We identified multiple druggable oncogene fusions, including those involving the *NRG1*, *ERBB4*, and *BRAF* genes, in invasive mucinous adenocarcinoma (IMA), a malignant type of LDAC. The fusions occurred mutually exclusively with *KRAS* mutations, a common driver oncogene aberration in IMA. These fusions represent potentially clinically relevant targets for treatment of IMAs that lack *KRAS* mutations.

Materials and Methods

Samples

Ninety IMAs were identified among consecutive patients with primary adenocarcinoma of the lung who were treated surgically at the National Cancer Center Hospital, Tokyo, Japan, from 1998 to 2013. Histologic diagnoses were based on the most recent World Health Organization classification and the International Association for the Study of Lung Cancer/American Thoracic Society/European Respiratory Society (IASLC/ATS/ERS) criteria for LADC (13, 17). Total RNA was extracted from grossly dissected, snap-frozen tissue samples using TRIzol (Invitrogen). The study was approved by the Institutional Review Boards of the participating institutions.

RNA sequencing

RNA sequencing libraries were prepared from 1 or 2 μg of total RNA using the mRNA-Seq Sample Prep Kit or TruSeq RNA Sample Prep Kit (Illumina). The resultant libraries were subjected to paired-end sequencing of 50 or 75 bp reads on a Genome Analyzer IIx (GAIIx) or HiSeq 2000 (Illumina). Fusion transcripts were detected using the TopHat-Fusion algorithm (18). Experimental conditions for RNA sequencing are described in Supplementary Table S1.

Examinations of oncogenic properties of fusion products

To construct lentiviral vectors for expression of the CD74-NRG1, EZR-ERBB4, and TRIM24-BRAF fusion proteins, full-length cDNAs were amplified from tumor cDNA by PCR and inserted into pLenti-6/V5-DEST plasmids (Invitrogen). The integrity of each inserted cDNA was verified by Sanger sequencing. Expression of fusion products of the predicted sizes was confirmed by Western blot analysis of transiently transfected and virally infected cells (Supplementary Fig. S1A). Details of plasmid transfection, viral infection, Western blot analysis, and soft agar colony and tumorigenicity assays are described in Supplementary Materials and Methods.

Results and Discussion

We prepared an IMA cohort of 90 cases consisting of 56 (62%) cases with *KRAS* mutations and 34 (38%) cases without. The 34 *KRAS*-negative cases included two, one, and one cases with *BRAF* mutation, *EGFR* mutation, and *EML4-ALK* fusion, respectively; the remaining 30 were "pan negative" for representative driver aberrations in LADCs. Thirty-two cases, consisting of 27 pan-negative and five *KRAS* mutation-positive cases, were subjected to RNA sequencing (Supplementary Table S1). Analysis of $>2 \times 10^7$ paired-end reads obtained by RNA sequencing and subsequent validation by Sanger sequencing of reverse transcription PCR (RT-PCR) products revealed five novel gene-fusion transcripts detected only in the pan-negative IMAs: *CD74-NRG1*, *SLC3A2-NRG1*, *EZR-ERBB4*, *TRIM24-BRAF*, and *KIAA1468-RET* (Fig. 1A and B; Table 1; details in Supplementary Materials and Methods; Supplementary Fig. S2 and Supplementary Table S2). RT-PCR screening of these fusions in the remaining 58 IMAs that had not been subjected to RNA sequencing revealed one additional pan-negative case with the *CD74-NRG1* fusion. Thus, the *CD74-NRG1* fusion, detected in five of 34 (14.7%) cases negative for *KRAS* mutations, was the most frequent fusion among *KRAS* mutation-negative IMAs. Fusions of *CD74* or *SLC3A2* with *NRG1* were present in 17.6% (6/34) of cases. The five novel fusions were mutually exclusively with one another and were not present in any of the *KRAS* mutation-positive cases (Table 2).

Four of the novel fusions, *CD74-NRG1*, *SLC3A2-NRG1*, *EZR-ERBB4*, and *TRIM24-BRAF*, involved rearrangements of genes encoding protein kinases or a ligand of a receptor protein kinase (NRG1/neuregulin/heregulin) for which oncogenic rearrangements have not been previously reported in lung cancer (Supplementary Fig. S3). The remaining fusion was a novel type involving the *RET* oncogene; fusions with *RET* are observed in 1% to 2% of LADCs (4, 5, 7, 8, 11). In a screen of 315 LADCs without IMA features from Japanese patients and 144 consecutive LADCs from U.S. patients, all tumors were negative for all of the *NRG1*, *BRAF*, and *ERBB4* fusions, as well as the novel *RET* fusion. Therefore, these fusions might be driver aberrations specific to LADCs with IMA features. The four novel gene fusions were likely to have been caused by interchromosomal translocations or paracentric inversion (Table 1 and Supplementary Fig. S3). Consistently, separation of the signals generated by the probes flanking the translocation sites of *NRG1* in fusion-positive tumors was observed upon FISH analysis of *CD74-NRG1* fusion-positive tumors (Supplementary Fig. S4). We also confirmed overexpression of NRG1, ERBB4, and BRAF proteins in tumor cells carrying the corresponding fusions by immunohistochemical analysis, using antibodies recognizing polypeptides retained in the fusion proteins; expression of NRG1, ERBB4, and BRAF proteins was also observed in some fusion-negative cases (Supplementary Fig. S5). IMAs harboring gene fusions were obtained from both male and female patients, although

Published OnlineFirst April 11, 2014; DOI: 10.1158/1078-0432.CCR-14-0107

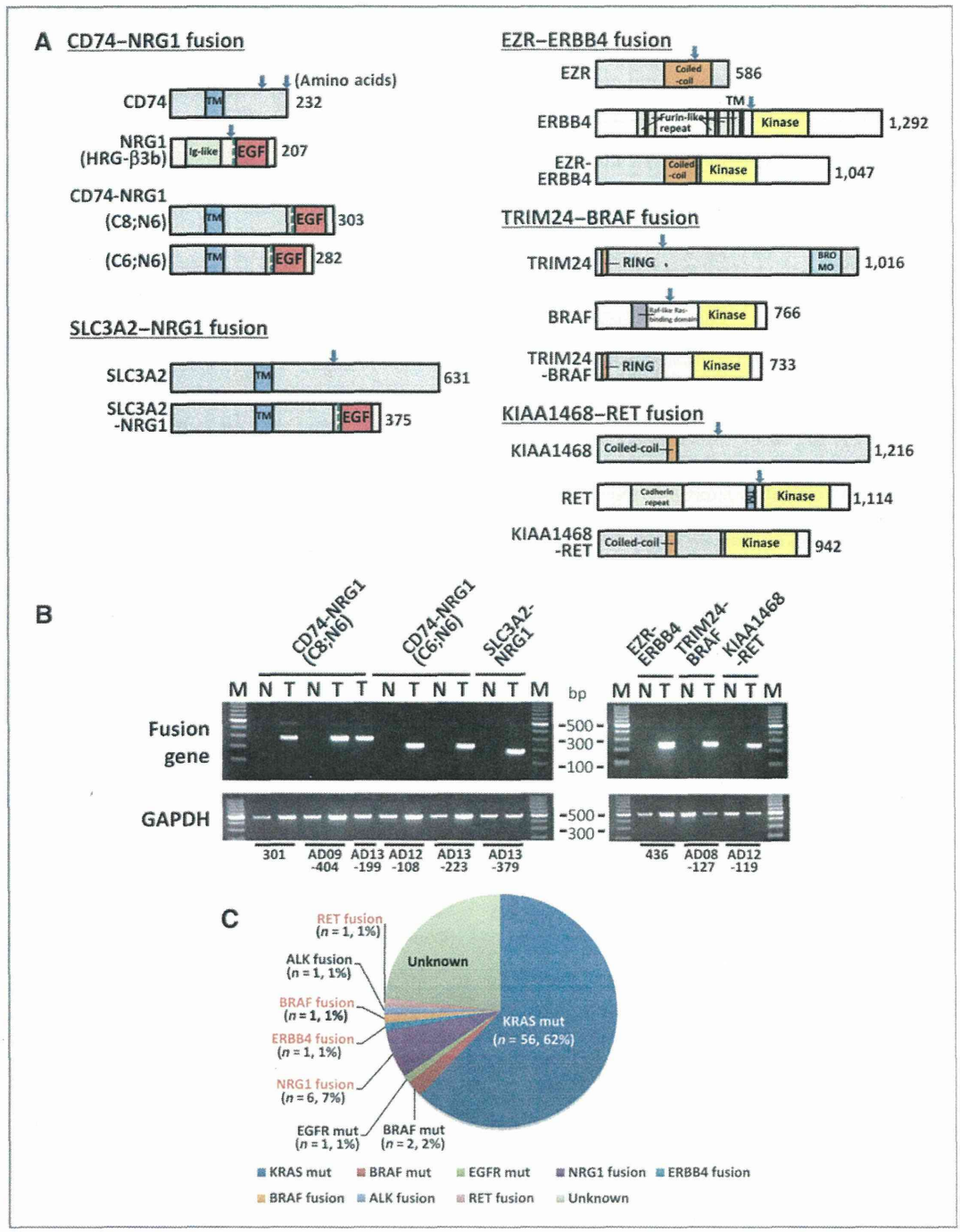

Figure 1. Oncogenic fusions in invasive mucinous LDAC. A, schematic representations of the wild-type proteins (top rows of each section) followed by the fusion proteins identified in this study. The breakpoints for each variant are indicated by blue arrows. TM, transmembrane domain. Locations of putative cleavage sites in the NRG1 polypeptide are indicated by dashed green lines. B, detection of gene-fusion transcripts by RT-PCR. RT-PCR products for glyceraldehyde-3-phosphate dehydrogenase (*GAPDH*) are shown below. Six IMAs (T) positive for gene fusions are shown alongside their corresponding non-cancerous lung tissues (N); labels below the gel image indicate sample IDs (see Table 1). C, pie chart showing the fraction of IMAs that harbor the indicated driver mutations.

Published OnlineFirst April 11, 2014; DOI: 10.1158/1078-0432.CCR-14-0107

Table 1. Characteristics of invasive mucinous LDACs with novel gene fusions

No.	Sample	Sex	Age	Smoking (pack/year)	Gene fusion	Chromosome aberration	Oncogene mutation[a]	Pathologic stage	TTF1	HNF4A
1	301T	M	55	Ever (47)	*CD74-NRG1*	t(5;8)(q32;p12)	None	1a	−	+
2	AD12-108T	F	68	Never	*CD74-NRG1*		None	2b	−	+
3	AD09-404T	F	78	Never	*CD74-NRG1*		None	1a	−	+
4	AD13-199T	F	47	Never	*CD74-NRG1*		None	1b	−	+
5	AD13-223T	F	53	Never	*CD74-NRG1*		None	1a	−	+
6	AD13-379T	F	66	Never	*SLC3A2-NRG1*	t(8;11)(p12;q13)	None	1b	Not tested	Not tested
7	436T	M	61	Ever (41)	*EZR-ERBB4*	t(2;6)(q25;q34)	None	1b	−	+
8	AD08_127T	F	66	Never	*TRIM24-BRAF*	inv7(q33;q34)	None	1a	+	+
9	AD12-119T	M	62	Current (63)	*KIAA1468-RET*	t(10;18)(q21;q11)	None	1a	+	−

[a]*EGFR*, *KRAS*, *BRAF*, and *HER2* mutations and *ALK*, *RET*, and *ROS1* fusions.

NRG1 fusion-positive cases were preferentially from female never smokers (Table 1).

The CD74-NRG1 and SLC3A2-NRG1 fusion proteins, whose sequences were deduced from RNA sequencing data, contained the CD74 or SLC3A2 transmembrane domain and retained the EGF-like domain of the NRG1 protein (NRG1 III-β3 form; Fig. 1A). The NRG1 III-β3 protein has a cytosolic N-terminus and a membrane-tethered EGF-like domain, and mediates juxtacrine signals signaling through HER2:HER3 receptors (19). Because parts of CD74 or SLC3A2 replaced the transmembrane domain of wild-type NRG1 III-β3, we speculated that the membrane-tethered EGF-like domain might activate juxtacrine signaling through HER2:HER3 receptors. In addition, it was also possible that expression of these fusion proteins resulted in the production of soluble NRG1 protein due to proteolytic cleavage at sites derived from NRG1 (dashed green lines in Fig. 1A), as recently suggested for NRG1 type III proteins (20, 21). Exposing EFM-19 cells to conditioned media from H1299 human lung cancer cells expressing exogenous CD74-NRG1 fusion protein resulted in phosphorylation of endogenous ERBB2/HER2 and ERBB3/HER3 proteins, suggesting that autocrine HER2:HER3 signaling was activated by secreted NRG1 ligands generated from CD74-NRG1 polypeptides (Fig. 2A). Phosphorylation of extracellular signal—regulated kinase (ERK) and AKT, downstream mediators of HER2:HER3, was also elevated. HER2, HER3, and ERK phosphorylation was suppressed by lapatinib and afatinib, U.S. Food and Drug Administration (FDA)-approved tyrosine kinase inhibitors (TKI) that target HER kinases (22–24). Together, these observations indicate that *NRG1* fusions activated HER2:HER3 signaling by juxtacrine and/or autocrine mechanisms.

The EZR-ERBB4 fusion protein contained the EZR coiled-coil domain, which functions in protein dimerization, and also retained the full ERBB4 kinase domain (Fig. 1A). These features indicated that the EZR-ERBB4 protein is likely to form a homodimer via the coiled-coil domain of EZR, causing aberrant activation of the kinase function of ERBB4, similar to the situation of *EZR-ROS1* fusion (5). Indeed, when the *EZR-ERBB4* cDNA was exogenously expressed in NIH3T3 fibroblasts, tyrosine 1258, located in the activation loop of the ERBB4 kinase site, was phosphorylated in the absence of serum stimulation, indicating that fusion with EZR aberrantly activated the ERBB4 kinase (Fig. 2B). Consistent with this, phosphorylation of a downstream

Table 2. Characteristics of 90 invasive mucinous LDACs

		Mutation			Fusion					
Variable	All	*KRAS*	*BRAF*	*EGFR*	*CD74-NRG1 or SLC3A2-NRG1*	*EZR-ERBB4*	*TRIM24-BRAF*	*EML4-ALK*	*KIAA1468-RET*	None (%)
Total	90 (100)	56 (62.2)	2 (2.2)	1 (1.1)	6 (6.7)	1 (1.1)	1 (1.1)	1 (1.1)	1 (1.1)	21 (23.3)
Age (mean ± SD; y)	67.2 ± 9.7	68.1 ± 9.7	66.5 ± 3.5	50	61.2 ± 11.5	61	66	64	62	68.1 ± 9.6
Sex										
Male (%)	39 (43.3)	28 (50.0)	0 (0)	0 (0)	1 (16.7)	1 (100)	0 (0)	0 (0)	1 (100)	8 (38.1)
Female (%)	51 (56.7)	28 (50.0)	2 (100)	1 (100)	5 (83.3)	0 (0)	1 (100)	1 (100)	0 (0)	13 (61.9)
Smoking habit										
Never smoker (%)	51 (56.7)	29 (51.8)	2 (100)	1 (100)	4 (66.7)	0 (0)	1 (100)	1 (100)	0 (0)	13 (61.9)
Ever smoker (%)	39 (43.3)	27 (48.2)	0 (0)	0 (0)	2 (33.3)	1 (100)	0 (0)	0 (0)	1 (100)	8 (38.1)

Published OnlineFirst April 11, 2014; DOI: 10.1158/1078-0432.CCR-14-0107

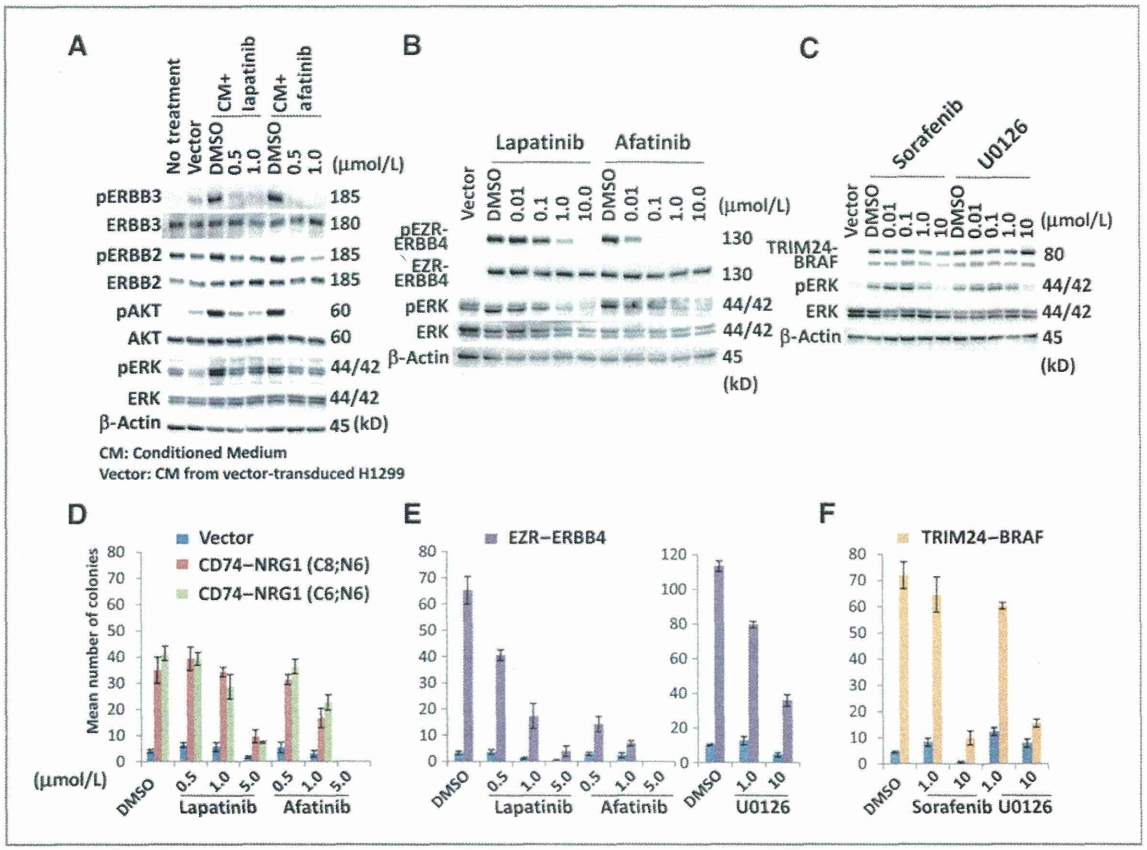

Figure 2. Oncogenic properties of gene-fusion products. A, ERBB3 activation by *CD74-NRG1* fusion, demonstrated using the EFM-19 cell system. ERBB3, ERBB2, AKT, and ERK phosphorylation were examined in EFM-19 (reporter) cells treated for 30 minutes with conditioned media from H1299 cells exogenously expressing *CD74-NRG1* cDNA. Phosphorylation was suppressed by HER-TKIs. B, ERBB4 activation by *EZR-ERBB4* fusion. Stably transduced NIH3T3 cells were serum-starved for 24 hours and treated for 2 hours with DMSO (vehicle control) or TKIs. Phosphorylation of ERBB4 and ERK was suppressed by ERBB4-TKIs. EZR-ERBB4 protein was detected using an antibody recognizing ERBB4 polypeptides retained in the fusion protein. C, BRAF activation by *TRIM24-BRAF* fusion. Stably transduced NIH3T3 cells were serum-starved for 24 hours and treated for 2 hours with DMSO or kinase inhibitors. ERK phosphorylation (activation) was suppressed by sorafenib, a kinase inhibitor targeting BRAF, as well as by U0126, a MEK inhibitor. TRIM24-BRAF protein was detected using an antibody recognizing BRAF polypeptides retained in the fusion protein. D–F, anchorage-independent growth of NIH3T3 cells expressing *CD74-NRG1* (D), *EZR-ERBB4* (E), or *TRIM24-BRAF* (F) cDNA, and suppression of this growth by kinase inhibitors. Mock-, *CD74-NRG1*-, *EZR-ERBB4*-, and *TRIM24-BRAF*–transduced NIH3T3 cells were seeded in soft agar with DMSO alone or kinase inhibitors. Colonies > 100 μm in diameter were counted after 14 days. Column graphs show mean numbers of colonies ± SEM.

mediator ERK was also elevated. Phosphorylation of ERBB4 and ERK was suppressed by lapatinib and afatinib, which inhibit ERBB4 protein (22–24).

The TRIM24-BRAF fusion protein retained the BRAF kinase domain but lacked the N-terminal RAS-binding domain responsible for negatively regulating BRAF kinase. These features suggested that the fusion was constitutively active, as in the cases of the *ESRP1-BRAF* and *AGTRAP-BRAF* fusions in other cancers (25). When the *TRIM24-BRAF* cDNA was exogenously expressed in NIH3T3 cells, ERK, a downstream mediator of BRAF, was phosphorylated in the absence of serum stimulation, indicating that fusion with TRIM24 aberrantly activated BRAF kinase (Fig. 2C). ERK phosphorylation was suppressed by sorafenib, an FDA-approved drug originally identified as a RAF kinase inhibitor (26), and also by the MEK inhibitor U0126 (Fig. 2C).

Exogenous expression of fusion gene cDNAs induced anchorage-independent growth of NIH3T3 fibroblasts, indicating their transforming activities (Fig. 2D–F). This growth was suppressed by the kinase inhibitors that suppressed fusion-induced activation of signal transduction, as described above. NIH3T3 cells expressing *EZR-ERBB4* or *TRIM24-BRAF* fusion cDNA formed tumors in nude mice (Fig. 3). Therefore, we concluded that these three fusions function as driver mutations in IMA development. We screened 200 commonly used human lung cancer cell lines, but all were negative for these three fusions (data not shown); thus, the oncogenic properties of these fusions remain unvalidated in human cancer cells.

Published OnlineFirst April 11, 2014; DOI: 10.1158/1078-0432.CCR-14-0107

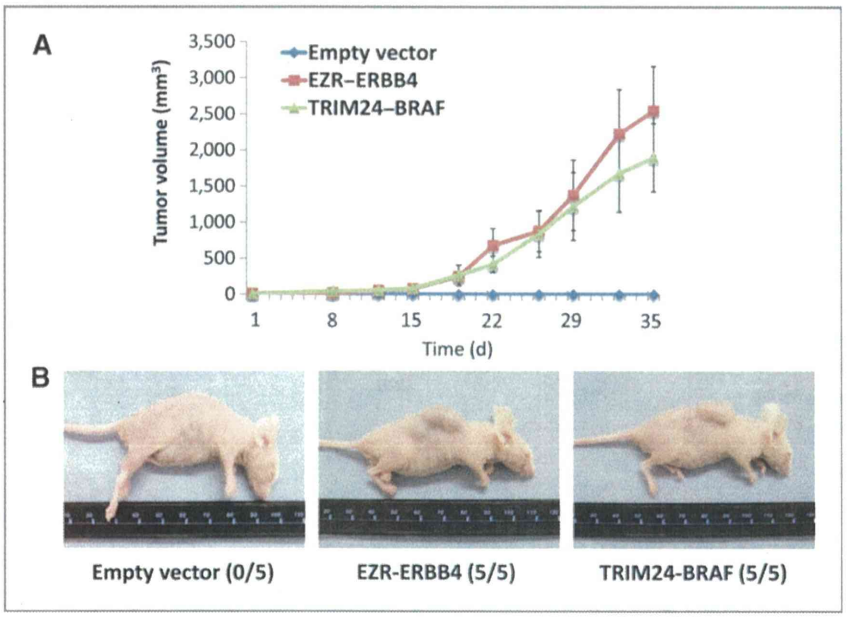

Figure 3. Tumorigenicity of NIH3T3 cells expressing *ERZ-ERBB4* or *TRIM24-BRAF* fusion cDNAs. A, tumor growth in nude mice injected with NIH3T3 cells expressing empty vector, *EZR-ERBB4* fusion, or *TRIM24-BRAF* fusion. Cells were resuspended with 50% Matrigel and injected into the right flank of nude mice. Tumor size was measured twice weekly for 5 weeks. Data are shown as mean ± SEM. B, representative tumors were photographed on day 21. The numbers in parentheses indicate the ratio of the number of mice with tumors to the number of mice receiving cell injection.

The results here suggest that the *NRG1*, *ERBB4* and *BRAF* fusions are novel driver mutations involved in the development of IMAs of the lungs (Fig. 1C) and potential targets for existing TKIs. The recurrent *NRG1* fusions were especially notable because NRG1 was previously identified as a regulator of goblet-cell formation in primary cultures of human bronchial epithelial cells (27); therefore, activation of the NRG1-mediated signaling pathway (s) might play a part in IMA development by contributing to both cell transformation and acquisition of goblet-cell morphology. In addition to a small fraction of known druggable aberrations (an *ALK* fusion and an *EGFR* mutation), more than 10% (11/90; 12.2%) of IMAs harbored other druggable aberrations targeted by existing kinase inhibitors: these aberrations were represented by fusions involving *NRG1*, *ERBB4*, *BRAF*, or *RET*, or *BRAF* mutations (Table 2, Fig. 1C). To facilitate translation of these findings to the cancer clinic, it will be necessary to establish diagnostic methods, particularly using break-apart and fusion FISH methods, capable of detecting these aberrations. Such methods will also help identify additional fusions involving other partner genes and contribute to a greater understanding of the significance of gene fusions in lung carcinogenesis.

Disclosure of Potential Conflicts of Interest

No potential conflicts of interest were disclosed.

Authors' Contributions

Conception and design: K. Tsuta, J. Yokota, T. Yoshida, T. Kohno
Development of methodology: H. Ichikawa
Acquisition of data (provided animals, acquired and managed patients, provided facilities, etc.): T. Nakaoku, K. Tsuta, H. Ichikawa, H. Sakamoto, K. Furuta, Y. Shimada, S.-I. Watanabe, H. Nokihara, K. Yasuda, M. Hiramoto, T. Nammo, T. Ishigame, H. Okayama
Analysis and interpretation of data (e.g., statistical analysis, biostatistics, computational analysis): T. Nakaoku, K. Tsuta, M. Enari, A.J. Schetter, C.C. Harris
Writing, review, and/or revision of the manuscript: T. Nakaoku, K. Tsuta, H. Ogiwara, S.-I. Watanabe, H. Nokihara, K. Yasuda, M. Hiramoto, A.J. Schetter, C.C. Harris, Y.H. Kim, M. Mishima, T. Yoshida, T. Kohno
Administrative, technical, or material support (i.e., reporting or organizing data, constructing databases): K. Tsuta, K. Shiraishi, M. Enari, H. Ogiwara, S.-I. Watanabe, H. Okayama
Study supervision: K. Tsuta, J. Yokota

Acknowledgments

The authors thank Suenori Chiku and Hirohiko Totsuka for the analysis of sequencing data and Dai Suzuki, Kazuko Nagase, Sachiyo Mitani, Sumiko Ohnami, Yoko Odaka, and Misuzu Okuyama for technical assistance.

Grant Support

This work was supported, in part, by the Advanced Research for Medical Products Mining Program of the National Institute of Biomedical Innovation (NIBIO), Grants-in-Aid from the Ministry of Health, Labor, and Welfare for the Third-term Comprehensive 10 year Strategy for Cancer Control and for Research for Promotion of Cancer Control Programs; and the Princess Takamatsu Cancer Research Fund.

The costs of publication of this article were defrayed in part by the payment of page charges. This article must therefore be hereby marked *advertisement* in accordance with 18 U.S.C. Section 1734 solely to indicate this fact.

Received January 14, 2014; revised March 22, 2014; accepted April 1, 2014; published OnlineFirst April 14, 2014.

References

1. Pao W, Hutchinson KE. Chipping away at the lung cancer genome. Nat Med 2012;18:349–51.
2. Shaw AT, Engelman JA. ALK in lung cancer: past, present, and future. J Clin Oncol 2013;31:1105–11.
3. Gautschi O, Zander T, Keller FA, Strobel K, Hirschmann A, Aebi S, et al. A patient with lung adenocarcinoma and RET fusion treated with vandetanib. J Thorac Oncol 2013;8:e43–4.

Published OnlineFirst April 11, 2014; DOI: 10.1158/1078-0432.CCR-14-0107

4. Drilon A, Wang L, Hasanovic A, Suehara Y, Lipson D, Stephens P, et al. Response to Cabozantinib in Patients with RET Fusion-Positive Lung Adenocarcinomas. Cancer Discov 2013;3:630–5.
5. Takeuchi K, Soda M, Togashi Y, Suzuki R, Sakata S, Hatano S, et al. RET, ROS1 and ALK fusions in lung cancer. Nat Med 2012;18:378–81.
6. Mano H. ALKoma: a cancer subtype with a shared target. Cancer Discov 2012;2:495–502.
7. Lipson D, Capelletti M, Yelensky R, Otto G, Parker A, Jarosz M, et al. Identification of new ALK and RET gene fusions from colorectal and lung cancer biopsies. Nat Med 2012;18:382–4.
8. Kohno T, Ichikawa H, Totoki Y, Yasuda K, Hiramoto M, Nammo T, et al. KIF5B-RET fusions in lung adenocarcinoma. Nat Med 2012; 18:375–7.
9. Ju YS, Lee WC, Shin JY, Lee S, Bleazard T, Won JK, et al. A transforming KIF5B and RET gene fusion in lung adenocarcinoma revealed from whole-genome and transcriptome sequencing. Genome Res 2012;22:436–45.
10. Oxnard GR, Binder A, Janne PA. New targetable oncogenes in non-small-cell lung cancer. J Clin Oncol 2013;31:1097–104.
11. Kohno T, Tsuta K, Tsuchihara K, Nakaoku T, Yoh K, Goto K. RET fusion gene: Translation to personalized lung cancer therapy. Cancer Sci 2013;104:1396–400.
12. Travis WD, Brambilla E, Riely GJ. New pathologic classification of lung cancer: relevance for clinical practice and clinical trials. J Clin Oncol 2013;31:992–1001.
13. Travis WD, Brambilla E, Noguchi M, Nicholson AG, Geisinger KR, Yatabe Y, et al. International association for the study of lung cancer/american thoracic society/european respiratory society international multidisciplinary classification of lung adenocarcinoma. J Thorac Oncol 2011;6:244–85.
14. Tsuta K, Kawago M, Inoue E, Yoshida A, Takahashi F, Sakurai H, et al. The utility of the proposed IASLC/ATS/ERS lung adenocarcinoma subtypes for disease prognosis and correlation of driver gene alterations. Lung Cancer 2013;81:371–6.
15. Warth A, Muley T, Meister M, Stenzinger A, Thomas M, Schirmacher P, et al. The novel histologic International Association for the Study of Lung Cancer/American Thoracic Society/European Respiratory Society classification system of lung adenocarcinoma is a stage-independent predictor of survival. J Clin Oncol 2012;30:1438–46.
16. Yoshizawa A, Motoi N, Riely GJ, Sima CS, Gerald WL, Kris MG, et al. Impact of proposed IASLC/ATS/ERS classification of lung adenocarcinoma: prognostic subgroups and implications for further revision of staging based on analysis of 514 stage I cases. Mod Pathol 2011;24:653–64.
17. Travis WD, Brambilla E, Muller-Hermelink HK, Harris CC, editors. World Health Organization classification of tumors: Pathology and genetics, tumours of lung, pleura, thymus and heart. Lyon, France: IARC Press; 2004.
18. Kim D, Salzberg SL. TopHat-Fusion: an algorithm for discovery of novel fusion transcripts. Genome Biol 2011;12:R72.
19. Falls DL. Neuregulins: functions, forms, and signaling strategies. Exp Cell Res 2003;284:14–30.
20. Fleck D, van Bebber F, Colombo A, Galante C, Schwenk BM, Rabe L, et al. Dual cleavage of neuregulin 1 type III by BACE1 and ADAM17 liberates its EGF-like domain and allows paracrine signaling. J Neurosci 2013;33:7856–69.
21. Dislich B, Lichtenthaler SF. The membrane-bound aspartyl protease BACE1: molecular and functional properties in Alzheimer's disease and beyond. Front Physiol 2012;3:8.
22. Majem M, Pallares C. An update on molecularly targeted therapies in second- and third-line treatment in non-small cell lung cancer: focus on EGFR inhibitors and anti-angiogenic agents. Clin Transl Oncol 2013;15:343–57.
23. Perez EA, Spano JP. Current and emerging targeted therapies for metastatic breast cancer. Cancer 2012;118:3014–25.
24. Nelson V, Ziehr J, Agulnik M, Johnson M. Afatinib: emerging next-generation tyrosine kinase inhibitor for NSCLC. Onco Targets Ther 2013;6:135–43.
25. Palanisamy N, Ateeq B, Kalyana-Sundaram S, Pflueger D, Ramnarayanan K, Shankar S, et al. Rearrangements of the RAF kinase pathway in prostate cancer, gastric cancer and melanoma. Nat Med 2010; 16:793–8.
26. Wilhelm SM, Adnane L, Newell P, Villanueva A, Llovet JM, Lynch M. Preclinical overview of sorafenib, a multikinase inhibitor that targets both Raf and VEGF and PDGF receptor tyrosine kinase signaling. Mol Cancer Ther 2008;7:3129–40.
27. Kettle R, Simmons J, Schindler F, Jones P, Dicker T, Dubois G, et al. Regulation of neuregulin 1beta1-induced MUC5AC and MUC5B expression in human airway epithelium. Am J Respir Cell Mol Biol 2010;42:472–81.

Published OnlineFirst April 11, 2014; DOI: 10.1158/1078-0432.CCR-14-0107

AACR American Association for Cancer Research

Clinical Cancer Research

Druggable Oncogene Fusions in Invasive Mucinous Lung Adenocarcinoma

Takashi Nakaoku, Koji Tsuta, Hitoshi Ichikawa, et al.

Clin Cancer Res 2014;20:3087-3093. Published OnlineFirst April 11, 2014.

PHLDA3 is a novel tumor suppressor of pancreatic neuroendocrine tumors

Rieko Ohki[a,1], Kozue Saito[a,b], Yu Chen[a,b], Tatsuya Kawase[c], Nobuyoshi Hiraoka[d], Raira Saigawa[a,b], Maiko Minegishi[a,b], Yukie Aita[a], Goichi Yanai[e], Hiroko Shimizu[f], Shinichi Yachida[a], Naoaki Sakata[g], Ryuichiro Doi[h], Tomoo Kosuge[i], Kazuaki Shimada[j], Benjamin Tycko[j], Toshihiko Tsukada[k], Yae Kanai[d], Shoichiro Sumi[e], Hideo Namiki[b], Yoichi Taya[c,l], Tatsuhiro Shibata[f,2], and Hitoshi Nakagama[a,2]

Divisions of [a]Refractory Cancer Research, [c]Radiobiology, [d]Molecular Pathology, [f]Cancer Genomics, and [k]Familial Cancer Research, National Cancer Center Research Institute, Tsukiji 5-1-1, Chuo-ku, Tokyo 104-0045, Japan; [b]Graduate School of Advanced Science and Engineering, Waseda University, 3-4-1 Okubo, Shinjuku-ku, Tokyo 169-8555, Japan; [e]Department of Organ Reconstruction, Institute for Frontier Medical Sciences, Kyoto University, 53 Kawahara-cho, Shogoin, Sakyo-ku, Kyoto 606-8507, Japan; [g]Division of Hepato-Biliary-Pancreatic Surgery, Department of Surgery, Tohoku University Graduate School of Medicine, 2-1, Seiryo-machi, Aoba-ku, Sendai 980-8575, Miyagi, Japan; [h]Department of Surgery and Surgical Basic Science, Graduate School of Medicine, Kyoto University, Yoshida-Konoe-cho, Sakyo-ku, Kyoto 606-8501, Japan; [i]Hepatobiliary and Pancreatic Surgery Division, National Cancer Center Hospital, Tsukiji 5-1-1, Chuo-ku, Tokyo 104-0045, Japan; [j]Institute for Cancer Genetics, Columbia University, New York, NY 10032; and [l]Cancer Research Center of Excellence, Center for Life Sciences, National University of Singapore, Singapore 117456

Edited by Douglas Hanahan, Swiss Federal Institute of Technology Lausanne, Lausanne, Switzerland, and approved May 1, 2014 (received for review October 25, 2013)

The molecular mechanisms underlying the development of pancreatic neuroendocrine tumors (PanNETs) have not been well defined. We report here that the genomic region of the *PHLDA3* gene undergoes loss of heterozygosity (LOH) at a remarkably high frequency in human PanNETs, and this genetic change is correlated with disease progression and poor prognosis. We also show that the *PHLDA3* locus undergoes methylation in addition to LOH, suggesting that a two-hit inactivation of the *PHLDA3* gene is required for PanNET development. We demonstrate that PHLDA3 represses Akt activity and Akt-regulated biological processes in pancreatic endocrine tissues, and that *PHLDA3*-deficient mice develop islet hyperplasia. In addition, we show that the tumor-suppressing pathway mediated by MEN1, a well-known tumor suppressor of PanNETs, is dependent on the pathway mediated by PHLDA3, and inactivation of PHLDA3 and MEN1 cooperatively contribute to PanNET development. Collectively, these results indicate the existence of a novel PHLDA3-mediated pathway of tumor suppression that is important in the development of PanNETs.

p53

Neuroendocrine tumors (NETs) arise from cells of the endocrine and nervous systems, and are found in tissues such as lung, pancreas and pituitary (1–3). NETs often produce, store and release biogenic amines and polypeptide hormones, and secretary granules containing these products provide a diagnostic marker for NETs. The mechanisms underlying the development of NETs remain unclear to date, due to the low incidence of these tumors and due to the lack of suitable experimental model systems, including genetically engineered mouse models. Pancreatic NET (PanNET), which is probably the best-studied NET, is the second-most common pancreatic tumor, having an incidence of ~1 per 100,000 individuals. Patients having late-stage PanNET often harbor tumors that are unresectable or metastatic and face limited treatment options. Accordingly, the prognosis of patients having metastatic PanNET is the worst among the NET subtypes, with a 5-y survival rate of 27–43% (1). Recently, the drug Everolimus has shown promise in the treatment of PanNETs (4), providing a significant improvement in progression-free survival. Everolimus is an inhibitor of mammalian target of rapamycin (mTOR), a downstream mediator of the PI3K/Akt pathway. The striking efficacy of Everolimus demonstrates the importance of the PI3K/Akt pathway in the pathology of PanNETs.

In agreement with these clinical results, studies on pancreatic endocrine cell lines have identified the PI3K/Akt signaling pathway as a major proliferation and survival pathway in these cells (5). Activated Akt phosphorylates substrates such as mTOR and controls various biological processes, including protein synthesis, proliferation, cell growth, and survival. Regulation of pancreatic islet β-cell proliferation, cell size, and apoptosis by Akt has been demonstrated using various mouse models. For example, transgenic mice overexpressing constitutively active Akt in β-cells exhibit increased β-cell proliferation and cell size and decreased induction of apoptosis (6).

Recently, the results of whole exomic sequencing of 10 PanNET specimens were published, revealing several key genetic alterations (7). In particular, genes in the PI3K/Akt pathway, i.e., TSC2, PTEN, and PIK3CA, were mutated in 15% of PanNETs. However, this represents only a subset of PanNETs, and may not fully explain the remarkable clinical results achieved by Everolimus in the majority of PanNET patients.

Previously, we have shown that PHLDA3 is a novel p53-regulated repressor of Akt. The PHLDA3 contains a PH domain that, we showed, competes with the PH domain of Akt for binding to membrane lipids, thereby inhibiting Akt translocation

Significance

Pancreatic neuroendocrine tumors (PanNETs) are a rare pathology, and molecular mechanisms underlying their development have not been well defined. This article shows that a two-hit inactivation of the *PHLDA3* gene is required for PanNET development: methylation of the locus and loss of heterozygosity. PHLDA3 functions as a suppressor of PanNETs via repression of Akt activity and downstream Akt-regulated biological processes. In addition, the tumor-suppressing pathway mediated by MEN1, a well known suppressor of PanNETs, is dependent on the pathway mediated by PHLDA3, and inactivation of PHLDA3 and MEN1 cooperatively contribute to PanNET development. Novel PHLDA3-mediated pathway of tumor suppression that is important in the development of PanNETs is demonstrated, and the findings may contribute to personalized medicine of PanNET patients.

Author contributions: R.O. designed research; R.O., K. Saito, Y.C., R.S., M.M., Y.A., and H.S. performed research; T. Kawase, N.H., G.Y., S.Y., N.S., R.D., T. Kosuge, K. Shimada, B.T., T.T., Y.K., S.S., H. Namiki, Y.T., T.S., and H. Nakagama contributed new reagents/analytic tools; R.O. analyzed data; and R.O. wrote the paper.

The authors declare no conflict of interest.

This article is a PNAS Direct Submission.

[1]To whom correspondence should be addressed. E-mail: rohki@ncc.go.jp.

[2]T.S. and H. Nakagama contributed equally to this work.

This article contains supporting information online at www.pnas.org/lookup/suppl/doi:10.1073/pnas.1319962111/-/DCSupplemental.

to the cellular membrane and its activation. We also showed that PHLDA3 may have a tumor suppressive function (8). However, there has hitherto been no reported role for PHLDA3 in human tumors, and its in vivo function has remained elusive. In this report, we demonstrate that the *PHLDA3* gene is a novel tumor suppressor, inactivation of which can lead to the development of PanNETs. We show that the *PHLDA3* genomic locus undergoes LOH and that the *PHLDA3* promoter is methylated at a high frequency in PanNETs. Furthermore, analysis of *PHLDA3*-deficient mice showed that these mice frequently develop islet hyperplasia as a result of enhanced islet cell proliferation and an increase in islet cell size. Collectively, these results indicate that PHLDA3 functions as a tumor suppressor in PanNETs.

Results

Frequent LOH at the *PHLDA3* Gene Locus in PanNETs. The *PHLDA3* gene is located at 1q31, a locus that has been reported to have a high frequency of LOH in two NETs derived from pancreas: insulinomas and gastrinomas (9, 10). We therefore speculated that the *PHLDA3* locus may undergo LOH in PanNETs, and analyzed the *PHLDA3* locus for LOH using microsatellite markers surrounding the gene in 54 PanNET samples (Fig. 1 *A–D*; clinical diagnosis for each sample is shown in *SI Appendix*, Fig. S1*A*). As shown in Fig. 1*B*, out of 54 PanNETs, 50 samples were informative and 36 samples showed LOH at the *PHLDA3* locus. The incidence of LOH at the *PHLDA3* locus (72%) is remarkably high, and was comparable to the reported LOH incidence of the *MEN1* gene, which has the highest reported incidence of genomic changes in PanNETs (11). Within the region analyzed, the LOH frequency peaks near the *PHLDA3* locus, suggesting that LOH of the *PHLDA3* gene is critical for PanNET development (Fig. 1*D*). This tendency becomes clearer when samples that exhibit partial LOH within this region (PanNET 1–18) were analyzed (Fig. 1*D*, blue line). A strikingly high incidence of LOH at the *PHLDA3* locus indicates the importance of this PHLDA3-regulated tumor suppression pathway in PanNETs. Most of the PanNETs analyzed in this study are nonfunctional, and we found no associations between *PHLDA3* LOH and specific PanNET type or insulin/glucagon positivity, to the extent that we examined this (*SI Appendix*, Fig. S1).

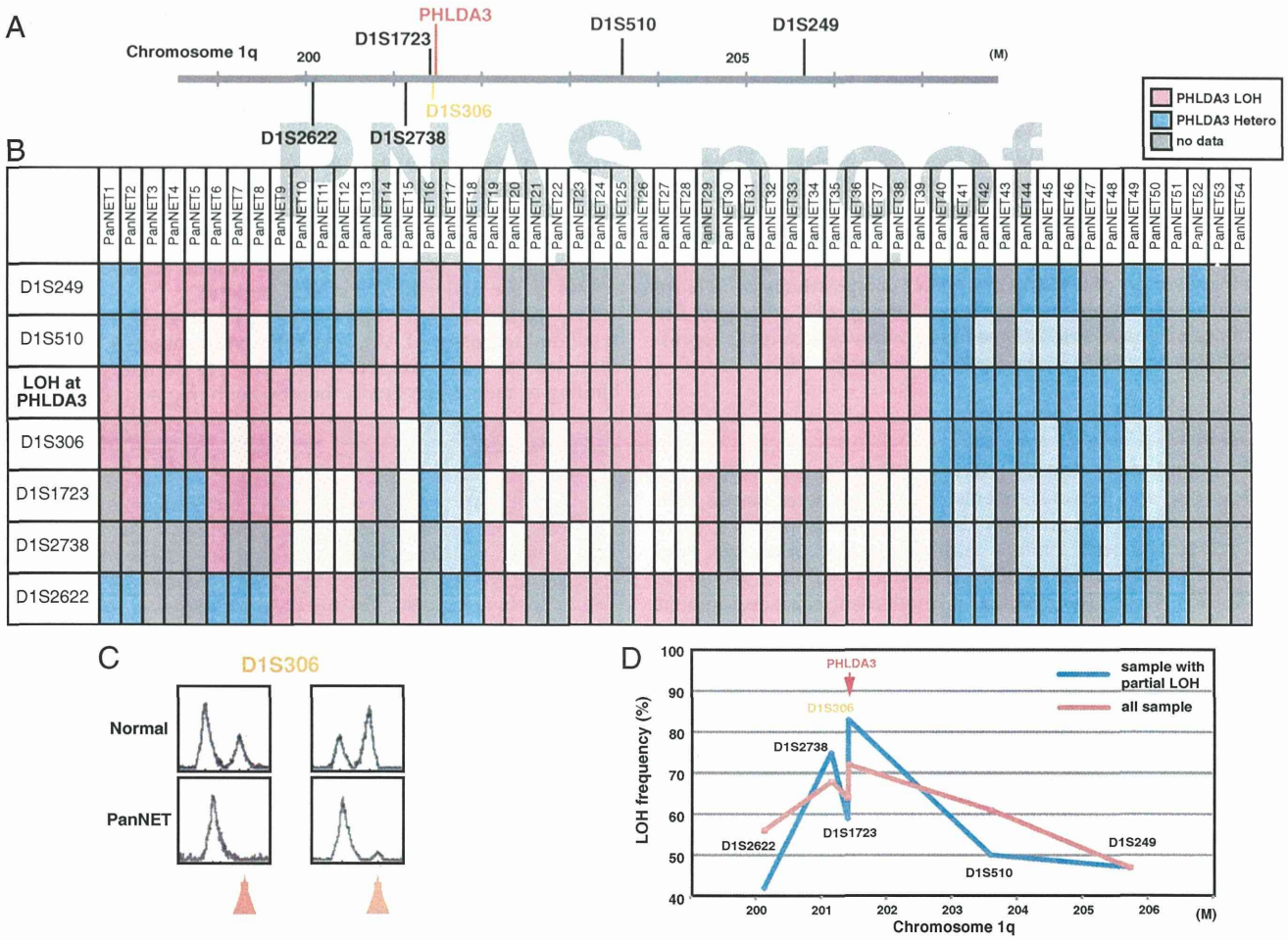

Fig. 1. Frequency of LOH at the *PHLDA3* gene locus in PanNETs. (*A*) Chromosomal locations of *PHLDA3* gene and microsatellite markers used in this study. D1S306 is located just next to the *PHLDA3* gene (32 kb upstream). (*B*) Microsatellite analysis of the *PHLDA3* gene locus region. PanNET samples were analyzed for LOH around the *PHLDA3* gene locus. Because D1S306 is located next to the *PHLDA3* gene, the LOH status of the *PHLDA3* gene was determined from the LOH status of the D1S306 locus. For some loci with no data (not informative or data unavailable), the LOH status of the locus was determined from the surrounding LOH status (shown in faint pink and faint blue). (*C*) Representative microsatellite analysis results. In normal tissues, two peaks derived from maternal and paternal alleles were detected, whereas in tumors, one allele was lost (shown by orange arrows), indicating LOH at the locus. (*D*) LOH frequency for each microsatellite marker. Frequencies from all samples (shown by red line) and frequencies from samples showing LOH partially within the analyzed region (PanNET1-18, shown by blue line) are shown.

PHLDA3 and MEN1 Cooperatively Suppress PanNET. The most outstanding genomic aberration previously reported in PanNETs was the mutation and LOH of the *MEN1* gene, a tumor suppressor gene associated with multiple endocrine neoplasia type 1 (7, 11). It has been reported that ~50% of PanNET cases exhibit LOH of the *MEN1* gene. Therefore, we analyzed whether *MEN1* LOH is observed in our PanNET samples. As shown in Fig. 2 *A* and *B*, 32 samples out of 48 informative samples showed LOH at the *MEN1* locus. Frequent LOH was observed at the *MEN1* locus in our samples (67%), confirming previous studies. We next combined the LOH data for the *PHLDA3* and *MEN1* loci. As shown in Fig. 2*C*, LOH at the *PHLDA3* and *MEN1* loci did not show a mutually exclusive pattern, which would be expected if PHLDA3 and MEN1 were on the same tumor suppressing pathway. Interestingly, we observed a significant frequency of double LOH, i.e., occurring at both the *PHLDA3* and *MEN1* loci (25 of 45 samples, $P < 0.05$ by Fisher's exact test). These data suggest that development of PanNET involves the functional loss of both pathways.

LOH at the *PHLDA3* Locus Is Correlated to Poor Prognosis in PanNET Patients. To select the proper treatment for each PanNET patient, prediction of disease prognosis is important. We observed that LOH at the *PHLDA3* locus was associated with advanced stage PanNETs, whereas absence of LOH was associated with lower tumor grades. These associations were statistically significant ($P < 0.01$, by Fisher's exact test), suggesting that the LOH is associated with a malignant phenotype in PanNETs (Fig. 3*A*). We next analyzed the relationship between LOH at the *PHLDA3* locus and the prognosis of PanNET patients. As shown in Fig. 3*B*, patients exhibiting LOH at the *PHLDA3* locus seemed to have a poorer prognosis compared with the patients without LOH. However, the observed difference did not achieve statistical significance, probably due to the relatively small numbers of patients analyzed. On the other hand, LOH at the *MEN1* locus had no influence on tumor grade or patient survival, as has been reported (7) (Fig. 3 *C* and *D*). It will be necessary to extend these studies with larger numbers of patients before reaching a firm conclusion, however these results suggest that the PHLDA3-regulated pathway, but not the MEN1-regulated pathway, may be a critical determinant of the prognosis of PanNET patients.

The *PHLDA3* Gene Undergoes Aberrant Methylation in Addition to LOH in PanNETs. Because we found frequent LOH at the *PHLDA3* locus in PanNETs, we next examined how the remaining allele is inactivated. The *PHLDA3* gene is mutated in several cancers: 11 mutations in lung, urinary, and large intestine cancer are reported in the COSMIC database (http://cancer.sanger.ac.uk/cancergenome/projects/cosmic), and mutation in lung cancer was reported by Yoo et al. (12). Therefore, we analyzed the *PHLDA3* ORF genomic sequence in our PanNET samples, but did not find any mutations within the coding regions (*SI Appendix*, Fig. S2). We next analyzed *PHLDA3* mRNA expression levels in these PanNETs. As shown in Fig. 4*A*, *PHLDA3* expression was significantly lower in samples showing LOH at the *PHLDA3* locus compared with samples without LOH. We noticed a CpG island overlapping the promoter region and the first exon of the *PHLDA3* gene (Fig. 4*B*). We therefore analyzed whether the methylation status of the *PHLDA3* gene is related to *PHLDA3* transcription levels. Specifically, we analyzed DNA methylation levels within the first exon of the *PHLDA3* gene, because it has been reported that methylation of the first exon is tightly linked to transcriptional silencing (13). Analysis of *PHLDA3* mRNA expression levels in four cancer cell lines revealed that *PHLDA3* is highly expressed in LNCaP and MDA-MB-M468 cells, whereas expression is very low in DLD1 and H1299 cells (Fig. 4*C*). Analysis

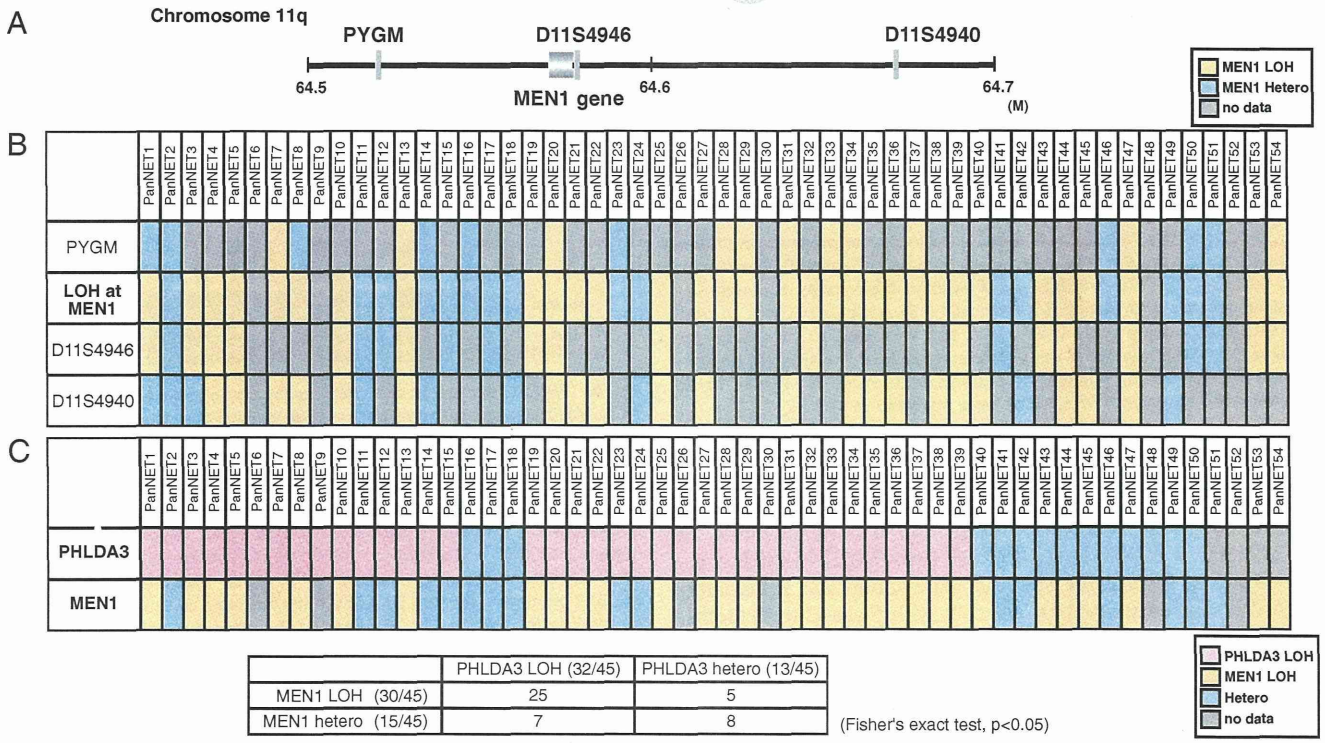

	PHLDA3 LOH (32/45)	PHLDA3 hetero (13/45)
MEN1 LOH (30/45)	25	5
MEN1 hetero (15/45)	7	8

(Fisher's exact test, $p<0.05$)

Fig. 2. Relationship between PHLDA3 and MEN1 tumor-suppressing pathways. (*A*) Chromosomal locations of the *MEN1* gene and microsatellite markers used in this study. (*B*) Analysis of LOH at the *MEN1* locus. The LOH status of the *MEN1* gene was determined from the LOH status of either of the informative markers. (*C*) Relationship between LOH status of the *PHLDA3* and *MEN1* loci. In total, 45 samples informative for both *PHLDA3* and *MEN1* loci were analyzed.